Apoptosis (2019) 24:758–772
https://doi.org/10.1007/s10495-019-01555-7

Aspirin induces oncosis in tumor cells

Lu Wang[1] · Zihao Mai[1] · Mengxin Zhao[2] · Bin Wang[1] · Si Yu[1] · Xiaoping Wang[2] · Tongsheng Chen[1]

Published online: 26 June 2019

Abstract
In contrast to the well-known anti-tumor mechanisms of aspirin in inducing apoptosis or autophagy, we here for the first time report oncosis induced by aspirin in tumor cells. In vitro and in vivo analysis showed that aspirin induced compromised Bcl-XL level and subsequent ATP depletion. Overexpression of CFP-Bcl-XL in Hela and A549 cells observably inhibited aspirin-induced ATP depletion and almost completely inhibited the aspirin-induced cells bubbling, while pharmacological inhibition of endogenous Bcl-XL activity by ABT-737 remarkably promoted aspirin-induced ATP depletion and cells bubbling, suggesting the key inhibitory role of Bcl-XL in aspirin-induced oncosis. Overexpression of Bax/Bad significantly promoted aspirin-induced oncosis. In addition, cells cultured in a glucose-free medium with low ATP level exhibited higher percentage of bubbling cells than the cells cultured in a glucose medium with high ATP level under aspirin treatment, indicating the important role of ATP depletion in aspirin-induced oncosis. Furthermore, caspase-3 was demonstrated to be not involved in aspirin-induced oncosis. Animal studies showed that aspirin treatment significantly inhibited tumors growth, but did not induce toxicities to mice. Collectively, aspirin inhibits tumors growth in mice and induces oncosis in which the compromised Bcl-XL and intracellular ATP depletion play a dominant role, which provides insights into the therapeutic strategy of aspirin in oncology.

Keywords Aspirin · Oncosis · Bcl-XL · ATP depletion · Caspase-3

Introduction

Aspirin, one of the three classic drugs in the history of medicine, is the most widely used nonsteroidal anti-inflammatory drug (NSAID) worldwide [1]. Aspirin was initially used to reduce inflammation, potent analgesic and anti-pyretic [2], and soon afterwards was opened for cardiovascular and cerebrovascular diseases [3, 4]. Furthermore, two large-scale clinical trials by International Stroke Trial (IST) and Chinese Acute Stroke Trial (CAST) have established the status of aspirin in the acute stage of stroke in 1997 [5, 6]. More interestingly, a lot of clinical studies have proved that aspirin can prevent a variety of tumors [7–10].

Aspirin has primarily been reported to inhibit tumor cells proliferation by inhibiting cyclooxygenase-2 enzyme (COX-2) and decreasing prostaglandins [11–14]. However, accumulating evidences have shown that COX-2 inhibition is not the only target of aspirin [15–18]. Intrinsic apoptotic factors including caspases, Bax and cytochrome c have been confirmed to play a critical role in aspirin-induced apoptosis [19–21]. Aspirin can also induce autophagy through AMPK/mTOR signaling pathway [22, 23].

Oncosis, a fashion of cell death, is characterized by cellular swelling, presence of dilatation organelles, and formation of plasma membrane protrusions called blebs [24–30]. ATP depletion is considered to be the initial step towards oncosis [31–34]. Moreover, Bcl-XL was proved to enhance ATP synthesis in hippocampal neurons [35]. Whether the Bcl-2 family proteins are involved in oncosis is controversial. Bcl-2 was reported to inhibit oncosis in GT1-7 cells treated with buthionine sulfoximine (BSO) or diethylmaleate

Electronic supplementary material The online version of this article (https://doi.org/10.1007/s10495-019-01555-7) contains supplementary material, which is available to authorized users.

✉ Xiaoping Wang
txp2938@jnu.edu.cn

✉ Tongsheng Chen
chentsh@scnu.edu.cn; chentsh126@126.com

[1] MOE Key Laboratory of Laser Life Science & College of Biophotonics, South China Normal University, Guangzhou 510631, China

[2] Department of Pain Management, The First Affiliated Hospital, Jinan University, Guangzhou 5610632, China

(DEM) [36], and Bax played an important role in acetaminophen (APAP) overdose-induced oncosis [37]. However, Bcl-2 was not involved in the oncosis induced by the increasing uncoupling protein 2 (UCP-2) in Hela cells [38], and Bax and caspase-3 were not involved in the calpain-induced renal cells oncosis [39, 40], which was further verified in sanguinarine-induced oncosis in CEM-VLB 1000 and CEM-T4 cell lines [41].

In this study, we demonstrated that aspirin induced oncosis in which Bcl-XL, an anti-apoptotic protein, plays a dominant role. Aspirin significantly inhibited tumors growth and induced oncosis in five tumor cell lines, and almost completely induced oncosis in Hela cells. Declined Bcl-XL level was critical in aspirin-induced oncosis, and aspirin decreased intracellular ATP level as a result of the decline of Bcl-XL level. In addition, Bax/Bad significantly promoted aspirin-induced oncosis in which caspase-3 was not involved. Our findings uncover a previously unknown but essential role of aspirin-induced oncosis in tumor treatment.

Materials and methods

Materials

Aspirin was from Solarbio (Bejing, China). Working solutions were prepared by dissolving the compounds in dimethylsulphoxide (DMSO, Sigma, USA) before experiments. The final concentration of DMSO was less than 0.4% in all experiments. Staurosporine (STS) and ATP Assay Kit were purchased from Beyotime (Shanghai, China). ABT-737 and Z-DEVD-FMK (caspase-3 specific inhibitor) were purchased from Merck-Calbiochem (USA). Rabbit monoclonal anti-Bcl-XL (54H6) and anti-caspase-3 (8G10), and mouse monoclonal anti-Tubulin antibody were purchased from Cell Signaling Technology (Beverly, MA, USA). Proper goat anti-mouse and goat anti-rabbit secondary antibodies were purchased from Invitrogen (Massachusetts, USA). Turbofect™ transfection regent was purchased from ThermoFisher Scientific (Massachusetts, USA).

Cell lines and cell culture

Hela cells, EMT6 cells and LO2 cells (a kind of human normal hepatocyte) were obtained from the Department of Medicine, Jinan University (Guangzhou, China). A549 cells were purchased from Cell Bank of CAS (Shanghai, China). HepG2 and Hep3B cells were purchased from the Experimental Animal Center, SUN YAT-SEN University (Guangzhou, China). SH-SY5Y cells were obtained from American Type Culture Collection. Cells were cultured in Dulbecco's Modified Eagle's Medium (DMEM, Gibco, Grand Island) supplemented with 10% fetal bovine serum (FBS, Sijiqing, Hangzhou, China), 1% penicillin and streptomycin (Gibco, Grand Island). Cells were maintained in a humidified incubator with 5% CO_2 at 37 °C.

Inhibitors treatment

For caspase-3 specific inhibitor (Z-DEVD-FMK) treatment, cells were preincubated with 30 μM Z-DEVD-FMK for 1 h before 16 mM aspirin treatment for indicated times; For Bcl-XL inhibitor (ABT-737) treatment, cells were treatment together with 10 μM ABT-737 and 16 mM aspirin, or treatment alone with 10 μM ABT-737 or 16 mM aspirin. All inhibitors were reconstituted in DMSO.

Cell viability assay

Cell viability was detected by Cell Counting Kit-8 (CCK-8, Dojindo, Japan) assay according to the manufacture's protocol as described previously [42]. Briefly, cells were seeded in 96-well plates at 1×10^4 per well for 24 h and subjected to the indicated treatments, viable cells were assessed by absorbance measurements at 450 nm using an auto microplate reader (infinite M200, Tecan, Austria). Results reflect the average of at least three replicates.

Characterization of cell death

Oncosis was characteristic with cell swelling with plasma membrane bubbling, pyknosis early in the bubbles with membrane integrity and karyolysis in later stage with loss of membrane integrity. Apoptosis was characteristic with cell shrinkage and circle, chromatin condensation, nuclear fragmentation, and the appearance of apoptotic bodies. Cells without apoptotic or oncosis features were considered viable. The numbers of normal, oncosis and apoptotic cells were calculated as a percentage of total cells.

The morphology of cells was analyzed by using a fluorescence microscope (Olympus IX73 equipped with a CCD camera, Japan). Nuclear morphology was analyzed by double staining with Hoechst 33258 and PI. In brief, cells were grown on the confocal dishes for 24 h. After being treated with indicated treatments, the cells were incubated with 20 μg/ml Hoechst 33258 for 30 min and then 10 μg/ml PI for 15 min at 37 °C in the dark. Cells were subsequently washed one time with PBS and visualized by fluorescence microscope.

Detection of subcellular distributions of GFP

Cells were transfected with 0.5 μg GFP using Turbofect™ transfection regent according to the manufacture's instructions. 24 h after transfection, cells were treated with aspirin for 12 or 24 h. Subcellular distributions of GFP were

visualized using a fluorescence microscope (Olympus IX73 equipped with a CCD camera, Japan). Excitation/emission wavelengths for GFP was 488/500–550 nm.

Transient transfection of FP-Bcl-2 proteins

After cells were seeded in 6-well plates or in confocal dishes and cultured overnight to reach 70–80% confluence at the day of transfection, the cells were transiently transfected with serum-free DMEM containing 0.25 μg CFP/YFP, CFP-Bcl-XL, CFP-Bax and YFP-Bad respectively using Turbofect™ transfection reagent, or cotransfected with serum-free DMEM containing 0.25 μg CFP-Bcl-XL and 0.5 μg YFP-Bad/YFP-Bax. 24 h after transfection, cells were treated with aspirin for indicate times and processed in the following experiments.

Measurement of mitochondrial membrane potential

JC-1 (Solarbio, Bejing, China), a mitochondrial membrane potential assay kit, was used to analyze loss of $\Delta\Psi_m$ by using FCM analysis. The dye molecules of J-aggregates in the mitochondria matrix and emit red fluorescence when mitochondria have high $\Delta\Psi_m$, and the dye molecules of JC-1 are monomer and emit green fluorescence when mitochondria have low $\Delta\Psi_m$ [43]. After 16 mM aspirin treatment for 12 and 24 h, the cells were stained with JC-1 (5 μg/ml) at 37 °C for 20 min in the dark and then washed with JC-1 staining buffer twice before FCM analysis. The excitation wavelength was 488 nm, and the emission wavelengths were 530/30 nm (to detect the monomer) and 630/22 nm (to detect the J-aggregates).

Western blotting analysis

Cells were collected and resuspended in ice-cold whole cell lysis buffer (10 mM Tris at pH 7.4, 1 mM NaF, 1 mM Na3VO4, 1 mM PMSF, 0.1% SDS, 1% Triton X-100, plus protease inhibitor cocktail). Equal amount of total protein, quantified by using the Bradford assay, were separated by SDS-PAGE electrophoresis and transferred on to polyvinylidene fluoride (PVDF) membranes according to standard techniques. Membranes were probed with the indicated primary antibodies overnight at 4 °C followed by incubation 1 h at room temperature with fluorescent secondary antibodies. Finally, the membranes were scanned using Odyssey Infrared Imaging System (LI-COR Biosciences, Nebraska, USA). Antibodies were used according to the manufacturer's recommendations. Tubulin was used as loading control.

Intracellular ATP detection

Intracellular ATP was measured with a commercial ATP detection kit (Beyotime, Shanghai, China) following the manufacturer's instructions. Cell cultured in 6-well plates were subjected to the indicated treatments, and collected and washed with PBS one time. For tumor tissues, use a glass homogenizer to fully homogenize, and the next steps are similar to that in cells. Intracellular ATP levels were taken as the luciferase activity using Luminescence (InfiniteM200, Tecan, Austria). Samples were normalized to protein concentration determined by using the BCA method.

Animal studies

Female Balb/c mice (6 weeks old) were obtained from Animal Experimental Center of Southern Medical University and approved by Guangdong Province Experimental Animals Monitoring Institute. EMT6 tumor bearing mice were established by subcutaneous injection of 5×10^6 cells in 125 μl PBS into the right flank region of Balb/c mice. The dimension of tumors was monitored by digital calipers. After tumor volumes reached approximately 60 mm^3, the mice were randomized into three different treatment groups (five mice per group): control group, vehicle (DMSO) group and aspirin group. The mice were injected intratumorally three times a week for 3 weeks with vehicle or aspirin (90 mg/kg/body weight) for vehicle and aspirin group respectively. After treatment, all mice were returned to animal housing and tumor volumes were tracked every 2 days by digital caliper measurements. The tumor volumes was calculated by formula $V = (\text{length} \times \text{width} \times \text{width})/2$. At the end of the study period, mice were euthanized and the tumors were fixed in 10% buffered formalin. Major organs of those mice were collected, fixed in 10% buffered formalin, conducted with paraffin embedded sections, stained with hematoxylin and eosin (H&E), and examined under a microscope.

Immunohistochemistry analysis

Tumor sections were dewaxed, rehydrated, and treated with 3% hydrogen peroxide, followed by antigen retrieval in boiling 0.1 M citrate (pH 6.0) buffer for 10 min twice. The sections were incubated with Bcl-XL antibody overnight at 4 °C and then incubated with a biotinylated secondary antibody for 50 min followed by incubation with horseradish peroxidase conjugated-avidin solution for 30 min. Finally, the nucleus were counterstained with hematoxylin. Bcl-XL staining in tumor cells were examined under a microscope.

Statistics

Data were presented as mean ± SD and analyzed using Student's *t* test. Statistical and graphic analyses were done using the software SPSS19.0 (SPSS, Chicago) and Origin 8.0 (Origin Lab Corporation). $P < 0.05$ was defined as statistical significance.

Results

Aspirin induces cytotoxicity in multiple tumor cell lines

We firstly used CCK-8 assay to assess the cytotoxicity of aspirin in four tumor cell lines (Hela, A549, Hep3B and SH-SY5Y). Treatment with different concentrations (8–16 mM) of aspirin for 24 h (Hela and A549 cells) or 48 h (Hep3B and SH-SY5Y cells) induced dose-dependent cytotoxicity (Fig. 1a). We next exposed Hela or A549 cells to 16 mM of aspirin for different times (0, 6, 12 18 and 24 h), and found that aspirin treatment induced time-dependent cytotoxicity in the two cell lines (Fig. 1b). Morphological analysis recorded using a digital camera (Sony, Japan) demonstrated that aspirin induced a time-dependent cell death (Fig. 1c). 16 mM aspirin was adopted in following experiments.

Aspirin induces oncosis

Microscopic imaging was used to explore the pattern of aspirin-induced cell death. Exposure of cells to aspirin for 24 h (Hela and A549 cells) or 48 h (SH-SY5Y, Hep3B and HepG2 cells) induced cytoplasmic swelling and plasma membrane bubbles in almost all Hela cells and most of other kinds of cells (A549, SH-SY5Y, Hep3B and HepG2) (Fig. 2a). Figure 2b shows the statistical fractions of bubbling, circular and surviving cells in Hela and A549 cell lines at the indicated times of aspirin treatment. Treatment with aspirin for 6, 12, 18 and 24 h respectively increased the proportions of bubbling cells from 0.85% (control) to 0.94, 12.718, 36.187 and 79.345% in Hela cells (Fig. 2b), and from 0.485% (control) to 0.52, 2.013, 38.86 and 54.733% in A549 cells (Fig. 2b). Aspirin treatment for 18 or 24 h markedly increased the percentage of bubbling cells, while the fractions of circular cells were as low as 1.129% and 0.184% in Hela cells, and 8.1% and 10.03% in A549 cells (Fig. 2b).

To find out the ingredients in the aspirin-induced plasma membrane bubbles, cells expressing GFP were imaged using fluorescence microscope. GFP distributed evenly in healthy cells, and was also observed in the aspirin-induced plasma membrane bubbles (Fig. 2c). To assess whether the aspirin-induced cytoplasm swelling were related to endoplasmic reticulum (ER), cells were expressed with ER-RFP plasmids, a specific ER probe [44]. We found that ER distribution was in net fashion in healthy cells, while ER was swelling and also observed in the bubbles in aspirin-treated

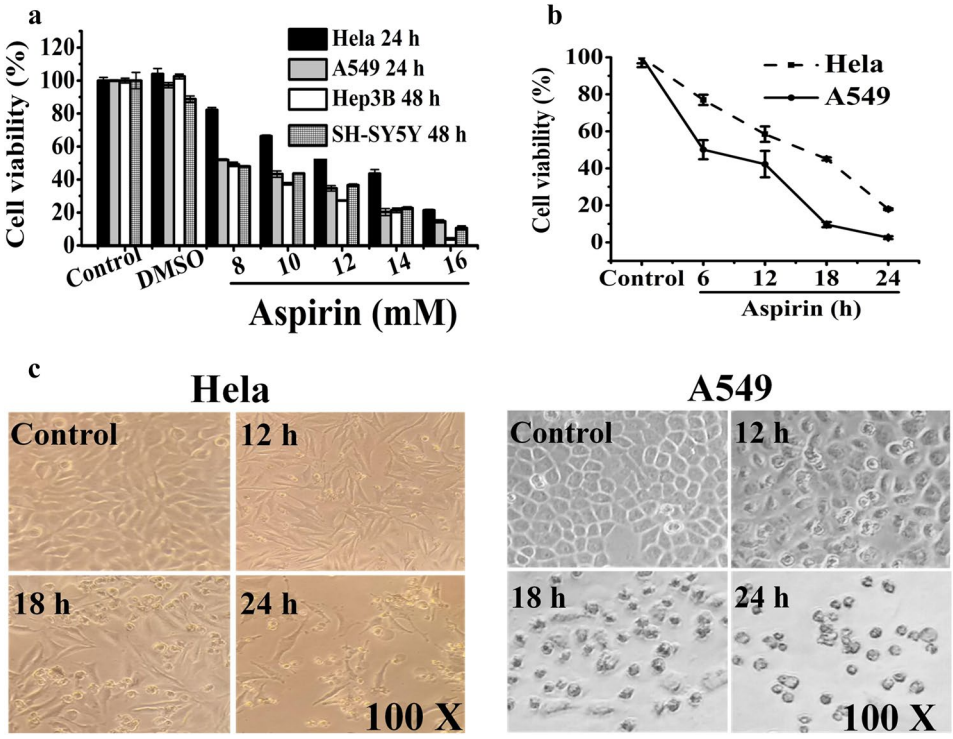

Fig. 1 Aspirin induces cytotoxicity in multiple tumor cell lines. **a, b** Aspirin induced dose-(**a**) and time (**b**)-dependent cytotoxicity measured by CCK-8 assay. Cells were seeded into 96-well microplate and incubated with different concentration of aspirin (0–16 mM) for 24 h or 48 h (**a**), or with aspirin (16 mM) for the indicated times (**b**). Data are from three independent experiments. **c** Morphological analysis on aspirin-induced cell death. Cells incubated with aspirin for 12, 18 and 24 h, respectively, were photographed with digital cameras on the inverted optical microscope. Magnification 100X

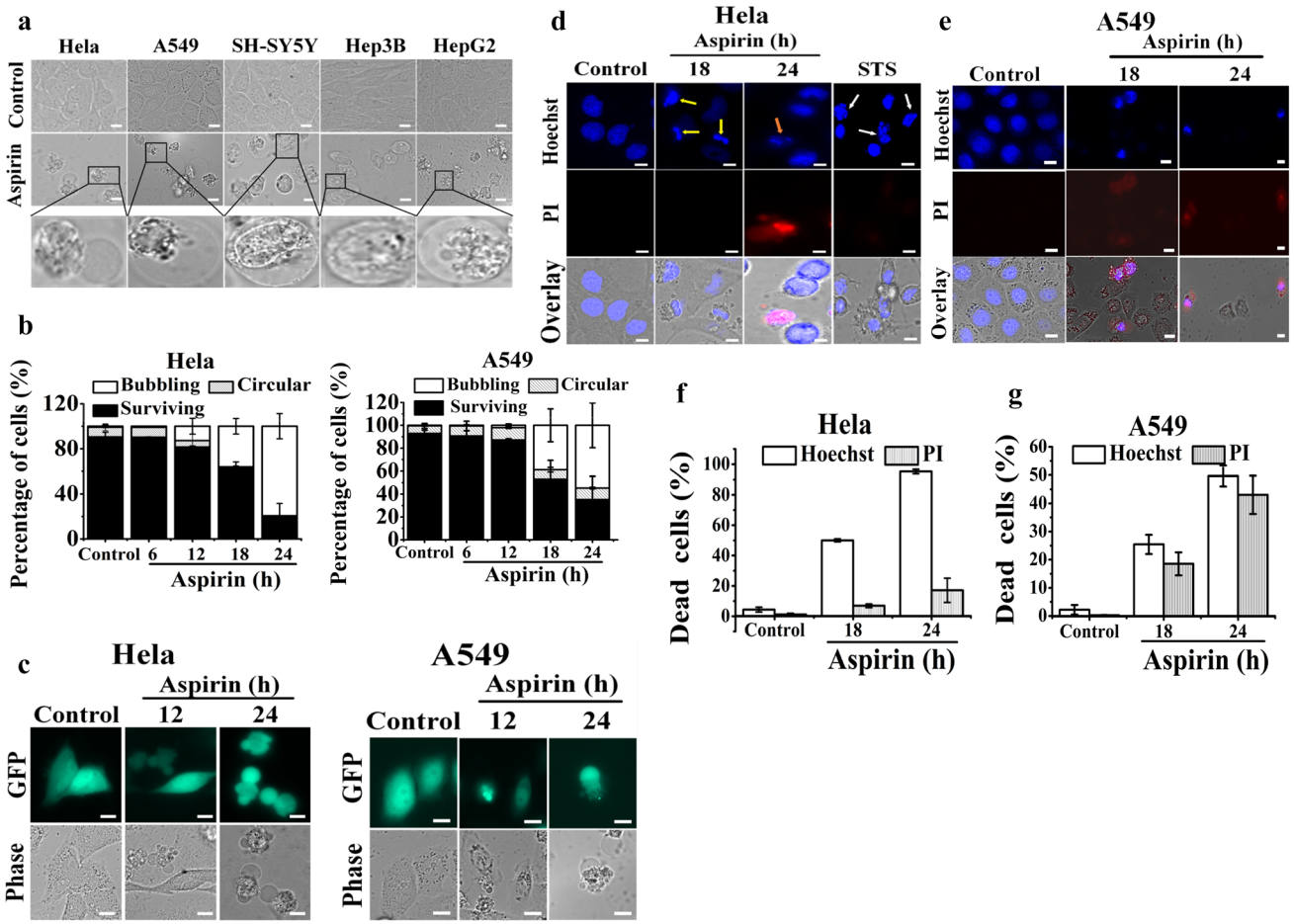

Fig. 2 Aspirin induces oncosis. **a** Representative bright field images of cells treated with 16 mM aspirin for 24 h (Hela/A549 cells) or 48 h (SH-SY5Y/Hep3B/HepG2 cells). The enlarged drawings show the bubbling cells. **b** Statistical percentages of bubbling, circular and surviving cells in Hela and A549 cells at the indicated times after aspirin treatment from at least 600 cells in three independent experiments. **c** Representative fluorescence and bright field images of Hela and A549 cells expressing GFP after treatment with 16 mM aspirin for the indicated times. **d, e** Representative Hoechst/PI fluorescence images and bright field images of Hela cells (**d**) and A549 cells (**e**). 1 μM STS treatment for 6 h was used to induce apoptosis. Yellow arrows indicate nucleus in the bubbles, orange arrow indicates karyolysis and white arrows indicate apoptotic bodies. **f** Statistical percentages of Hela cells with pyknosis/karyolysis and PI positive respectively from at least 300 cells in three independent experiments. **g** Statistical percentages of A549 cells with chromatin condensation and margination, and PI positive respectively from at least 200 cells in three independent experiments. Scale bar: 10 μm (Color figure online)

cells (Supplementary Fig. 1c). Furthermore, we used fluorescence microscope to image the mitochondria stained with mitotracker deep red, a probe for labelling mitochondria [45], and found that mitochondria were swelling but not observed in the bubbles after aspirin treatment (Supplementary Fig. 1d).

In order to verify whether aspirin induced apoptosis and necrosis in Hela cells, we imaged the cells probed by Hoechst 33258/PI staining. STS, an apoptotic positive drug, did induce pyknosis and apoptotic body formation (Fig. 2d). However, aspirin treatment for 18 h induced bright blue spot of Hoechst 33258 in the small bubbles (Fig. 2d), indicating that aspirin-induced plasma membrane bubbles were related to nucleus. Furthermore, at 24 h after aspirin treatment, nucleus were diffused and not observed in the big bubbles (Fig. 2d). Statistical results showed that the fraction of pyknosis or karyolysis cells determined by Hoechst 33258 imaging remarkably increased from 4.39% (control) to 50% and 95.2% at 18 and 24 h respectively after aspirin treatment (Fig. 2f). In order to determine whether aspirin induced necrosis, we examined the effect of aspirin on the disruption of cell membranes by PI staining (Fig. 2d), and found that the membrane of small bubbles (PI negative) were intact, indicating that aspirin induced oncosis instead of necrosis. Similar results were observed in A549 cells (Fig. 2e, g).

In order to figure out whether aspirin-induced oncosis was due to the acidic conditions but not aspirin in our experimental system, we used microscopic imaging to assess cells bubbling in A549 and Hela cells culturing in DMEM with the same pH value as the 16 mM aspirin, and

the measured results were in Supplementary Fig. 1a and b as follow. Firstly, we measured the pH value of DMEM medium and 16 mM aspirin by using pH Meter (Mettler Toledo, Switzerland), and the pH value were 8.5 and 7.1 respectively. We next adjusted pH value of DMEM medium to 7.1. Cells were cultured in DMEM medium 8.5 (control), DMEM medium 7.1 and 16 mM aspirin 7.1 respectively for 24 h, and then imaged as follow (Supplementary Fig. 1a). Culturing in DMEM medium 7.1 for 24 h did not significantly induce A549 and Hela cells bubbling (Supplementary Fig. 1a). Statistical results showed that the percentage of bubbling cells were 0.17% and 0% for A549 and Hela cells cultured in DMEM medium 7.1 for 24 h respectively while were 45.9% and 55.6% for A549 and Hela cells cultured in 16 mM aspirin 7.1 for 24 h respectively (Supplementary Fig. 1b), demonstrating that aspirin instead of acidic conditions induced oncosis.

Collectively, aspirin induces oncosis in tumor cells.

Caspase-3 is not involved in aspirin-induced oncosis

Cells stained with JC-1, a membrane-permeable dye [43], were used to evaluate the loss of mitochondrial membrane potential ($\Delta\Psi_m$) by FCM analysis. JC-1 fluorescence was seen primarily in Red channels and rarely in Green channels in control cells, and aspirin treatment for 12 and 24 h respectively significantly increased the percentage of cells with green fluorescence (Supplementary Fig. 2a). Statistical results showed that aspirin treatment for 12 and 24 h respectively increased the proportions of cells with green fluorescence from 16% (control) to 30% and 61% in Hela cells, and from 7% (control) to 17% and 60% in A549 cells (Fig. 3a), indicating that aspirin induced $\Delta\Psi_m$ loss early in 12 h.

We next used Western blotting analysis to assess whether aspirin induced caspase-3 cleavage in Hela and A549 cells. STS obviously decreased the level of pro-caspase-3 (Fig. 3b), indicating the cleavage of pro-caspase-3. Aspirin treatment for 12 h did not decrease the pro-caspase-3 level in Hela cells and modestly decreased the pro-caspase-3 level in A549 cells, and aspirin treatment for 24 h extensively decreased the pro-caspase-3 level (Fig. 3b). To further evaluate the role of caspase-3 in aspirin-induced oncosis, we next used CCK-8 assay to assess the effects of pretreatment with 30 μM Z-DEVD-FMK on the cytotoxicity of aspirin. Z-DEVD-FMK pretreatment significantly inhibited STS-induced cytotoxicity, but did not inhibit aspirin-induced cytotoxicity in Hela cells (Fig. 3c). Moreover, Z-DEVD-FMK pretreatment did not inhibit the aspirin-induced cells bubbling in Hela cells (Fig. 3d, Supplementary Fig. 2b).

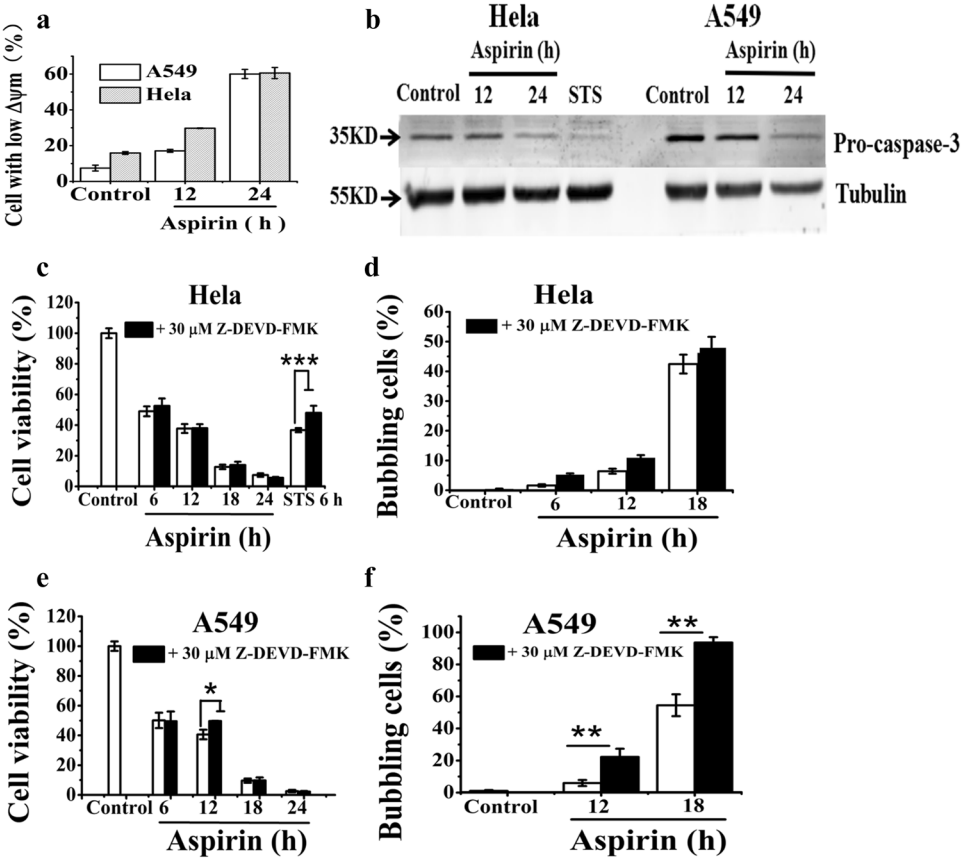

Fig. 3 Caspase-3 is not involved in aspirin-induced oncosis. **a** Aspirin induced $\Delta\Psi_m$ loss assessed by FCM analysis for the cells stained with JC-1 (5 μg/ml) probe after aspirin treatment for 12 and 24 h, respectively. **b** Level of pro-caspase-3 assessed by Western blotting for the cells treated with aspirin for 12 and 24 h, respectively. **c, d** Z-DEVD-FMK did not inhibit aspirin-induced cytotoxicity (**c**) and cells bubbling (**d**) in Hela cells. Cells treated with 1 μM STS for 6 h were used as positive control for cytotoxicity. **e, f** Z-DEVD-FMK significantly but modestly inhibited the aspirin-induced cytotoxicity (**e**) and significantly promoted aspirin-induced cells bubbling (**f**) in A549 cells. Cells were pretreated with Z-DEVD-FMK for 1 h before aspirin treatment. $^*P<0.05$, $^{**}P<0.01$ and $^{***}P<0.001$. Data are from three independent experiments

These data demonstrated that caspase-3 was not involved in aspirin-induced oncosis in Hela cells.

In A549 cells, although Z-DEVD-FMK pretreatment significantly but modestly inhibited the cytotoxicity of aspirin (Fig. 3e), this pretreatment did significantly increase the aspirin-induced cells bubbling (Fig. 3f, Supplementary Fig. 2c), indicating that caspase-3 was not involved in the aspirin-induced oncosis in A549 cells.

Key roles of Bcl-2 family proteins in aspirin-induced oncosis

To determine the role of Bcl-2 family proteins in aspirin-induced oncosis, cells expressing FP-Bcl-2 proteins were imaged using fluorescence microscope. Figure 4a shows the images of Hela cells separately expressing CFP, CFP-Bcl-XL, CFP-Bax and YFP-Bad, or coexpressing CFP-Bcl-XL and YFP-Bad or CFP-Bcl-XL and YFP-Bax in the presence or absence of aspirin. Expression of CFP-Bax or YFP-Bad observably increased the aspirin-induced cells death and bubbling, while expression of CFP-Bcl-XL significantly inhibited the aspirin-induced cells death and completely inhibited the aspirin-induced cells bubbling in the absence or presence of Bad or Bax (Fig. 4a). Figure 4b, c show the statistical percentages of aspirin-induced cell death (b) and cell bubbling (c) for the cells expressing FP-Bcl-2 family protein. We also did these experiments in A549 cells, and obtained similar results (Fig. 4d–f). In contrast to the complete contribution of CFP-Bax or YFP-Bad to the aspirin-induced bubbling in Hela cells (Fig. 4a), in the A549 cells expressing CFP-Bax or YFP-Bad, a few cells treated with aspirin died without characteristic of bubbling (Fig. 4d). Collectively, Bcl-2 family proteins play a key role in aspirin-induced oncosis: Bax and Bad enhances while Bcl-XL inhibits the aspirin-induced oncosis.

ATP depletion is involved in aspirin-induced oncosis

Oncosis pathways are often associated with compromised ATP levels [46]. We firstly evaluated the intracellular ATP level by using luminescence analysis with Microplate Reader (InfiniteM200, Tecan, Austria) for Hela and A549 cells cultured in a high glucose DMEM medium. Statistical results showed that aspirin treatment for 12 h induced a 34% of decrease in Hela cells (Fig. 5a) and 21% of decrease in A549 cells (Fig. 5b) in the relative ATP levels, indicating that aspirin treatment induced ATP depletion. Considering that the glucose in the medium was exploited by cells to synthesize ATP, we thus measured the ATP levels in Hela cells cultured in a glucose-free DMEM medium, and found that aspirin treatment for 12 h induced a 83% of decrease in the relative ATP level, much more than the aspirin-induced ATP decrease of cells cultured in high glucose DMEM (Fig. 5c). Moreover, extra adding 20 mM glucose to glucose-free DMEM medium (glucose DMEM medium) also significantly weaken the aspirin-induced ATP depletion (Fig. 5c). In order to figure out the relationship between aspirin-induced intracellular ATP depletion and oncosis, we imaged the Hela cells cultured in the glucose-free DMEM medium and glucose DMEM medium respectively at 12 h after aspirin treatment. Aspirin treatment for 12 h did not significantly induce cells bubbling for the Hela cells cultured in glucose DMEM medium but did observably induced cells bubbling for the cells cultured in glucose-free DMEM medium (Supplementary Fig. 3). Statistical results showed that the percentage of bubbling cells increased from 1.5% (control) to 36% for the cells cultured in glucose-free DMEM medium, much higher than the percentage (5.8%) of bubbling cells cultured in glucose DMEM medium (Fig. 5d), further demonstrating the important role of ATP depletion in aspirin-induced oncosis.

In A549 cells, aspirin treatment for 12 h did not obviously induce cells bubbling even in the cells cultured in glucose-free DMEM medium (data not shown). We thus assessed the effect of aspirin treatment for 18 h on cell bubbling, and found that the percentage of bubbling cells was up to 20% for the cells cultured in the glucose-free DMEM even without aspirin treatment (Fig. 5f), indicating the important role of glucose in cells bubbling. Aspirin treatment for 18 h also significantly increased the percentage of bubbling cells to 38% for the cells cultured in the glucose-free DMEM medium, much higher than the percentage of bubbling cells cultured in glucose DMEM medium (Fig. 5f).

Bcl-2 family proteins mediate aspirin-induced ATP depletion

Bcl-XL localizes in both the mitochondrial outer membrane and the inner membrane, and binds directly to the F_1 of F_1F_0 ATP synthase for improving metabolic efficiency by preventing the leakage of H^+ across the inner membrane [35, 47–49]. We firstly detected the effects of aspirin treatment on endogenous Bcl-XL level by Western blots analysis. As shown in Fig. 6a, aspirin treatment for 12 h decreased the total level of Bcl-XL but increased the phosphorylation Bcl-XL level (upper band), while aspirin treatment for 24 h significantly increased Bcl-XL level.

To assess the effect of Bcl-2 family proteins on aspirin-induced ATP depletion, we measured the intracellular ATP levels in the cells separately expressing CFP, CFP-Bcl-XL, CFP-Bax and YFP-Bad, or co-expressing CFP-Bcl-XL and YFP-Bad or CFP-Bcl-XL and YFP-Bax at 8 h after aspirin treatment, and found that overexpression of Bax/Bad markedly enhanced the aspirin-induced ATP depletion, while overexpression of Bcl-XL significantly inhibited the aspirin-induced ATP depletion in the absence or presence of Bad

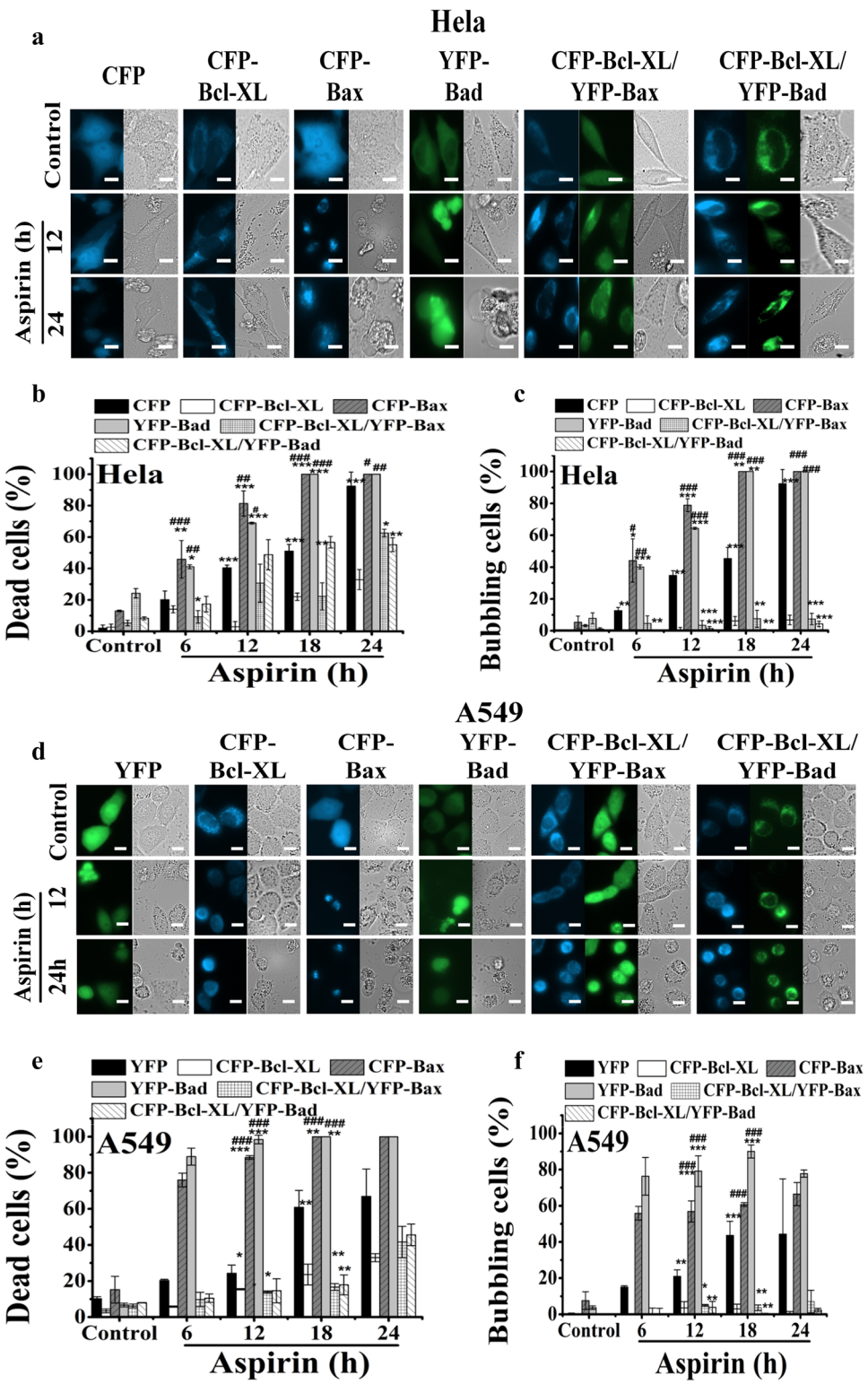

Fig. 4 Key roles of Bcl-2 family proteins in aspirin-induced oncosis. **a** Representative fluorescence and bright field images of Hela cells separately expressing CFP, CFP-Bcl-XL, CFP-Bax and YFP-Bad, or coexpressing CFP-Bcl-XL and YFP-Bax or CFP-Bcl-XL and YFP-Bad in the presence or absence of aspirin. Scale bar: 10 μm. **b** Bax/Bad significantly promoted but Bcl-XL significantly inhibited aspirin-induced cells death in Hela cells. **c** Bax/Bad significantly promoted but Bcl-XL completely inhibited aspirin-induced cells bubbling in Hela cells. Statistical percentages of dead or bubbling cells were from at least 800 cells in three independent experiments. **d**–**f** Similar results with **a**, **b** and **c** for A549 cells. $^{*}P < 0.05$, $^{**}P < 0.01$ and $^{***}P < 0.001$, compared with CFP or YFP; $^{\#}P < 0.05$, $^{\#\#}P < 0.01$ and $^{\#\#\#}P < 0.001$, CFP-Bax or YFP-Bad was compared with CFP-Bcl-XL/YFP-Bax or CFP-Bcl-XL/YFP-Bad

or Bax (Fig. 6b). To further assess the effect of endogenous Bcl-XL on aspirin-induced ATP depletion, we also assessed the effect of ABT-737, an analogue of BH3-only proteins that can inhibit the proapoptotic activity of Bcl-XL by direct binding [50], on the aspirin-induced ATP depletion at 12 h after aspirin treatment. ABT-737 markedly enhanced the aspirin-induced ATP depletion (Fig. 6c), indicating that inhibition of endogenous Bcl-XL by ABT-737 significantly promoted aspirin-induced ATP depletion. Furthermore, ABT-737 remarkably promoted aspirin-induced cells

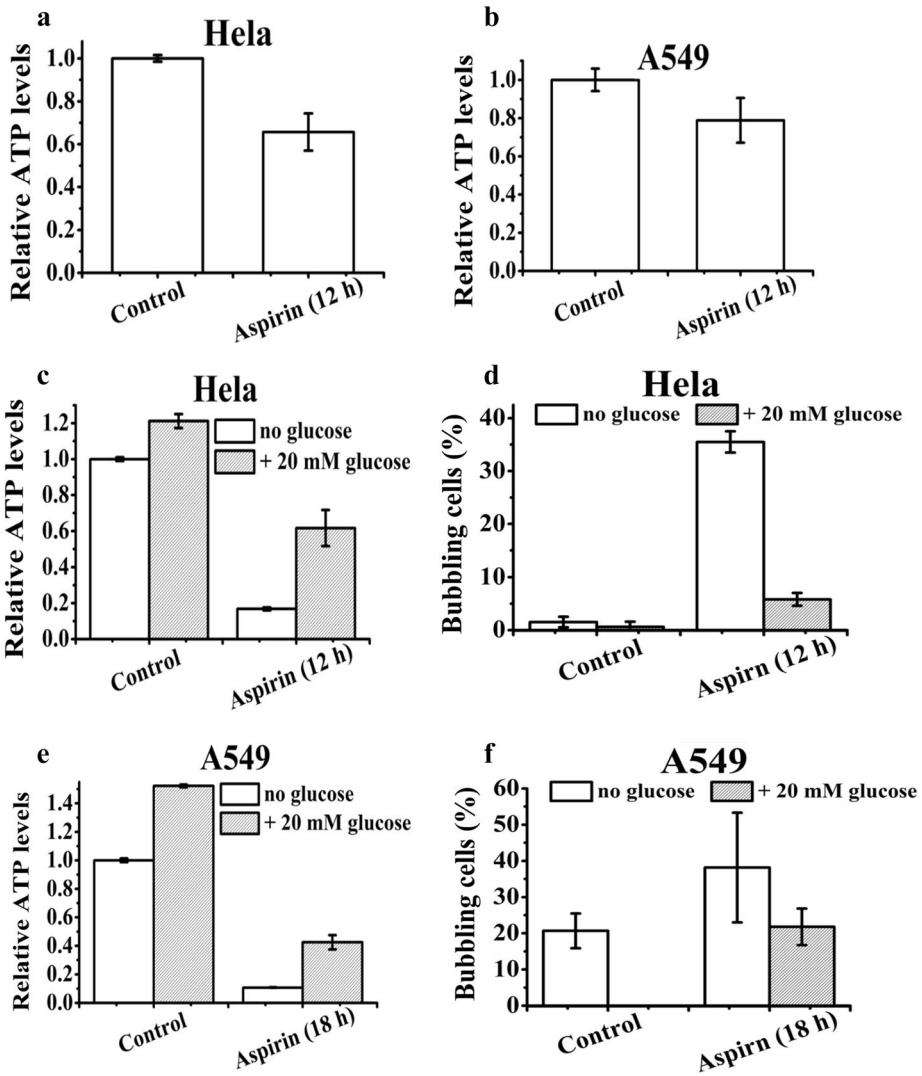

Fig. 5 ATP depletion is involved in the aspirin-induced oncosis. **a, b** Aspirin treatment for 12 h significantly induced ATP depletion in Hela (**a**) and A549 (**b**) cells cultured in high glucose DMEM medium. **c** Aspirin treatment for 12 h almost completely induced ATP depletion in Hela cells cultured in glucose-free DMEM medium. **d** Aspirin treatment for 12 h significantly induced cells bubbling in Hela cells cultured in glucose-free DMEM medium. Cells were cultured in glucose-free DMEM medium or glucose DMEM medium in the presence or absence of aspirin for 12 h. Statistical percentages of bubbling cells were from at least 300 cells in three independent experiments. **e, f** Similar results with **c** and **d** for A549 cells

bubbling (Fig. 6d, Supplementary Fig. 4a). Collectively, our data demonstrate that Bcl-XL plays a key role in aspirin-induced ATP depletion and oncosis.

Aspirin inhibits tumor growth in vivo

We next assessed the anti-tumor activity of aspirin in mice bearing breast cancer EMT6 tumors. Mice bearing EMT6 tumors were distributed into three groups and were treated according to the protocols summarized in "Materials and methods". In the next 3 weeks of treatment, the changes of tumor volumes and mice body weights were monitored every 2 days, and were plotted as a function of time after treatment (Fig. 7b, c). The photographs of the tested mice (before, on day 14, and day 21) were showed in Fig. 7a. As shown in Fig. 7b, the tumors of the mice in the DMSO group grew rapidly and had a similar volumes to control group, while the tumor volume of the mice in aspirin group was inhibited to a certain extent in the early 2 days, demonstrating that aspirin inhibited tumor growth in vivo.

Body weight is an important parameter to evaluate the toxicity of aspirin to mice. As shown in Fig. 7c, the body weight of the three groups had no obvious decrease, implying that treatment with aspirin had little adverse side effects. Subsequently, we carried out histological analysis to evaluate the potential side effects of aspirin on the major organs (heart, liver, spleen, lung and kidney) of mice. H&E staining histological sections showed no obvious histological lesion or any other tissue damage for the mice treated with aspirin (Fig. 7d), further indicating the safe application of aspirin in vivo.

Aspirin decreases the Bcl-XL and ATP level in tumor

Immunohistochemical staining of Bcl-XL in paraffin sections of EMT6 tumors showed that treatment of mice with aspirin resulted in an obvious decrease of Bcl-XL level

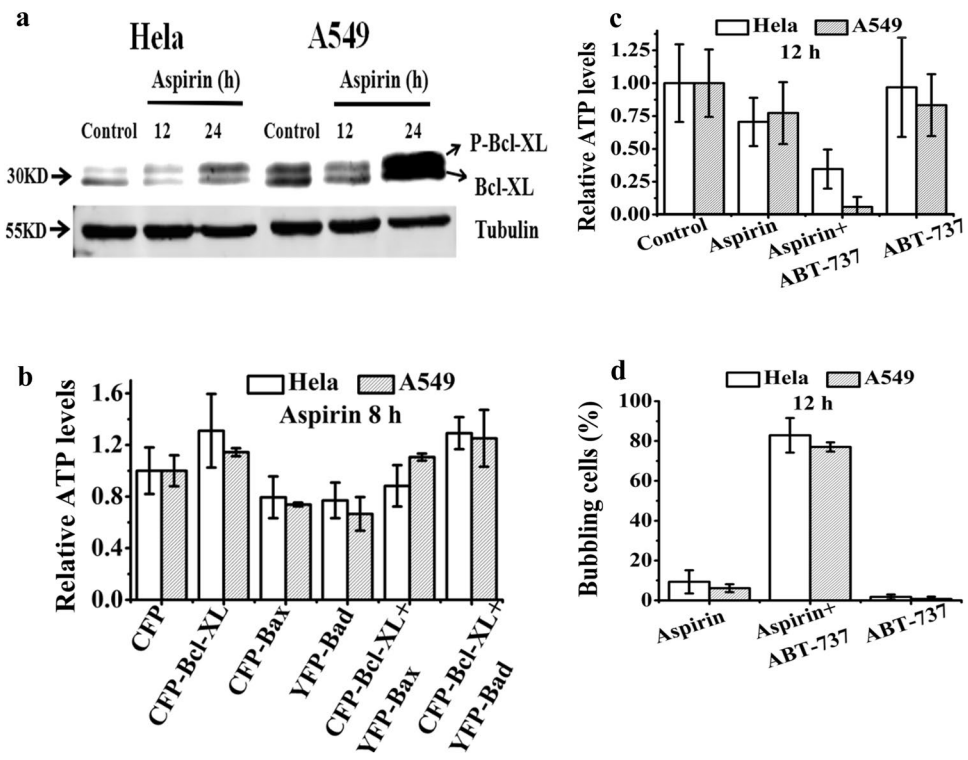

Fig. 6 Bcl-2 family proteins mediate aspirin-induced ATP depletion. **a** Effect of aspirin treatment on the level of Bcl-XL assessed by Western blotting. **b** Bax/Bad markedly enhanced but Bcl-XL markedly inhibited the aspirin-induced ATP depletion. **c** ABT-737 markedly enhanced the aspirin-induced ATP depletion. **d** ABT-737 remarkably promoted aspirin-induced cells bubbling. Statistical percentages of bubbling cells were from at least 300 cells in three independent experiments

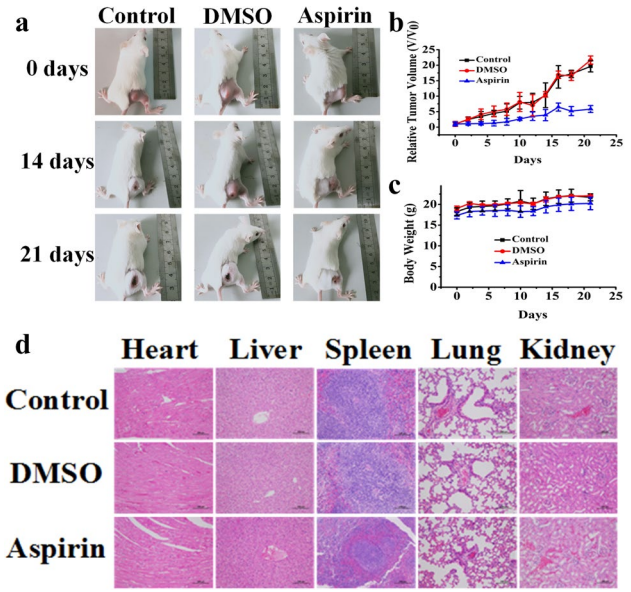

Fig. 7 Aspirin inhibits tumor growth in vivo. **a** Photographs of representative mice images before and after different times of aspirin treatment (before, on day 14, and day 21). **b** Aspirin treatment significantly inhibited the tumors growth. **c** Changes with time in body weight in control group, DMSO group and aspirin group respectively. **d** Representative H&E stained images of major organs including heart, liver, spleen, lung and kidney collected from mice. Scale bar: 100 μm

(Fig. 8a). Statistical results showed that aspirin treatment induced a 53.65% of decrease in the Bcl-XL level (Fig. 8b). We next evaluated the intracellular ATP level by using luminescence analysis with Microplate Reader, and found that aspirin treatment induced a 39% of decrease in the relative ATP level (Fig. 8c), indicating that aspirin treatment induced ATP depletion in tumor.

Discussion

Previous studies show that the common anti-tumor powers of aspirin are induction of apoptosis, autophagy and anti-proliferative activity [22, 51, 52]. Therefore, it was surprising to find that aspirin killed cells via oncosis, featuring with cell swelling and plasma membrane damage. Our data that aspirin treatment for 12 h did not induce caspase-3 cleavage, and extensive caspase-3 cleavage occurred at 24 h after aspirin treatment (Fig. 3b) indicate that caspase-3 cleavage is a consequence instead of the cause of the aspirin-induced oncosis. Moreover, Z-DEVD-FMK pretreatment did not inhibit aspirin-induced cytotoxicity and cells bubbling in Hela cells (Fig. 3c, d), further demonstrating that caspase-3 was not involved in aspirin-induced oncosis. Indeed, these data coincide with the notion that oncosis is caspase-3-independent [28, 53].

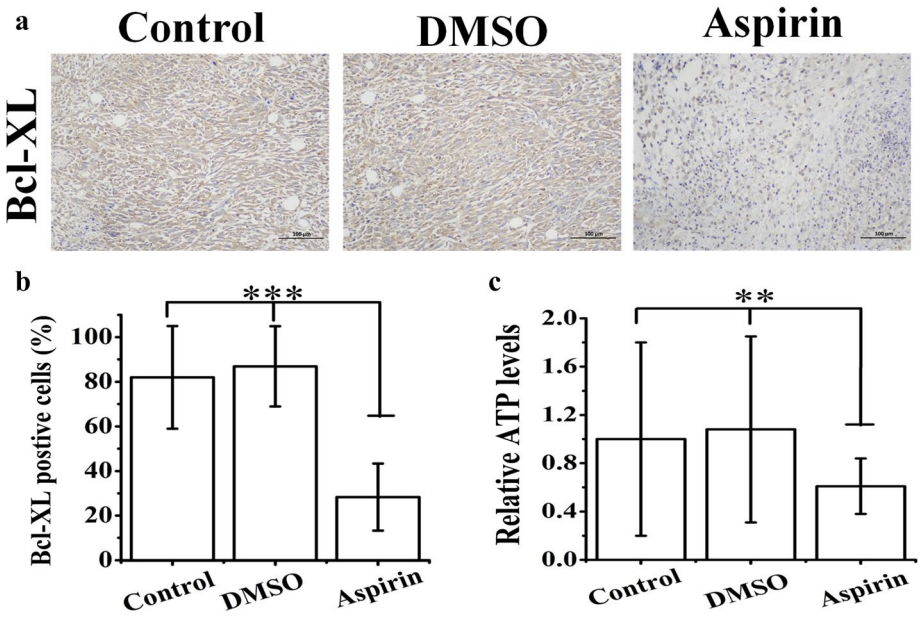

Fig. 8 Aspirin decreases the Bcl-XL and ATP level in tumor. **a** Representative results of immunohistochemistry against Bcl-XL on EMT6 tumors sections in control group, DMSO group and aspirin group respectively. Scale bar: 100 μm. **b** Quantification of immunohistochemistry on Bcl-XL positive cells in the tumors. Five visual fields were randomly selected and 100 cells in each visual field were counted. Bcl-XL positive staining shows brown color. Data are shown as the percentage of the hematoxylin staining cells (blue nucleus). **c** Aspirin treatment significantly induced ATP depletion in tumors. $^{*}P<0.05$, $^{**}P<0.01$ and $^{***}P<0.001$ (Color figure online)

Our data support the notion that ATP depletion is associated with oncosis. Although ATP is a critical component for the execution of apoptosis [54, 55], oncosis pathways are often associated with compromised ATP level [46]. The facts that aspirin treatment for 12 h induced ATP depletion (Fig. 5a, b) and cells began to bubble at 12 h and extensively bubbled at 18/24 h after aspirin treatment (Fig. 2b) indicate that ATP depletion may mediate aspirin-induced oncosis. Moreover, aspirin treatment also induced ATP depletion in the tumor of mice (Fig. 8c). Therefore, we speculated that because of the ATP depletion, the ATP level was not maintained at sufficient levels to drive caspase-3 activation (at 12 h), making the cells undergo oncosis instead of apoptosis. In addition, our data that the cells with low ATP level exhibited higher percentage of bubbling cells than the cells with high ATP level (Fig. 5c–f) further demonstrate the important role of ATP depletion in aspirin-induced oncosis.

The half-life of aspirin-induced ATP depletion delayed more than 12 h (Fig. 5a, b), which was contrast to the rapid decline (within 2 h) of intracellular ATP level induced by other positive oncosis inducers such as GSK1016790A [30]. Aspirin-induced gradual decline in intracellular ATP level may lead to asynchrony of tumor cells death, which may bestow therapeutic benefits, such as less likelihood of the development of tumor lysis syndrome (TLS) that is caused by rapid release of intracellular substances.

Our data that overexpression of CFP-Bcl-XL in Hela and A549 cells almost completely inhibited the aspirin-induced cells bubbling (Fig. 4) demonstrate the dominant inhibitory role of Bcl-XL in aspirin-induced oncosis, which is further verified by the fact that pharmacological inhibition of endogenous Bcl-XL activity by ABT-737 remarkably promoted aspirin-induced cells bubbling (Fig. 6d). It was reported that persistent opening of a voltage-sensitive channel formed by the c-subunit ring of the F_1F_0 ATP synthase led to permeability transition (PT) and cell death, while closure of the c-subunit channel promoted cell survival and increased efficiency of cellular metabolism [48]. Moreover, the β-subunit of F_1 can bind directly to the c-subunit of F_0 to inhibit pore activity, and physical uncoupling of F_1 from F_0 can increase conductance of the c-subunit's pore and then initiate PT [48]. Bcl-XL interacts directly with the β-subunit of the F_1F_0 ATP synthase and increases the efficiency of ATP synthesis by decreasing a proton leak within the F_1F_0 ATPase [35], which can be used to account for our data that overexpression of CFP-Bcl-XL significantly increases the intracellular ATP level (Fig. 6b) and pharmacological inhibition of endogenous Bcl-XL activity by ABT-737 remarkably decreases the intracellular ATP level (Fig. 6c). Our data that aspirin treatment for 12 h induces a decrease of total Bcl-XL level (Fig. 6a) and cells begin to bubble at the same time (Fig. 2a) further suggest a notion that aspirin-induced oncosis may be initiated by compromised Bcl-XL level, which was also verified by the in vivo analysis that aspirin inhibited EMT6 tumors growth in mice and also decreased the level of Bcl-XL and ATP in tumor (Fig. 8b, c). It is thus reasonable to infer that Bcl-XL inhibits aspirin-induced oncosis by increasing the efficiency of ATP synthesis.

Figure 9 shows a reasonable mechanism by which aspirin induces oncosis. In control cells, Bcl-XL binds to the β-subunit of F_1 to block the c-subunit's pore, the leaking channel of H^+, of F_0, leading to the reentry of H^+ into the mitochondrial matrix only via the a-subunit of F_0, which drives rotation of the central stalk against the catalytic F_1, which is required for ATP synthesis from ADP and pi [47]. In aspirin-treated oncosis cells, due to the functional inactivation

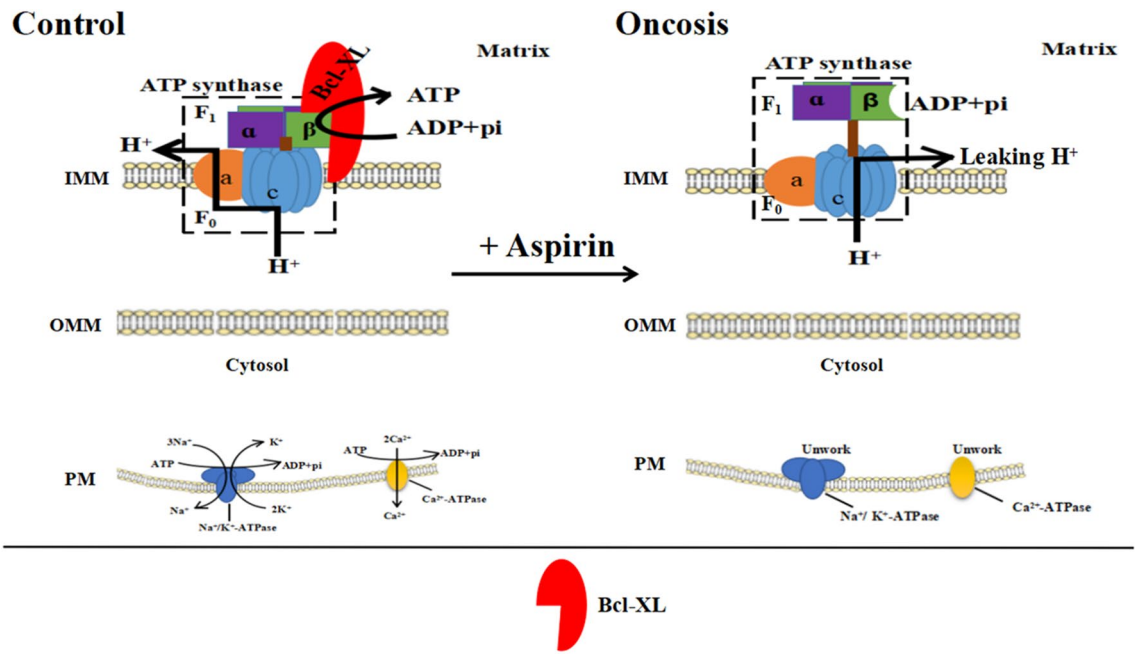

Fig. 9 Schematic on the mechanism of aspirin-induced oncosis

or decline of Bcl-XL, the β-subunit of F_1 is released from Bcl-XL, resulting in the open of the c-subunit's pore of F_0 and subsequent direct leakage of H^+ from the c-subunit's pore. In this manner, F_1F_0 ATP synthase can't work normally and thus ATP synthesis is blocked. Then, Na^+/K^+-ATPase and Ca^{2+}-ATPase at cell membrane do not work normally due to ATP depletion, resulting in an increase in Na^+, Cl^- and Ca^{2+} accompanied by water influx and cellular swelling [28].

Of course, another possibility is that aspirin induced compromised Bcl-XL level by decreasing the expression of Bcl-XL instead of increasing the degradation of Bcl-XL. Khandelwal et al. showed that aspirin induced the translocation of RelA/NF-κB from cytoplasm to nucleus, and the nucleolar RelA-mediated repression of NF-κB-driven transcription decreased Bcl-XL expression level [56]. In addition, active Mst1 phosphorylated Bcl-XL at Ser14, thereby antagonizing Bcl-XL-Bax binding and promoting apoptosis [57]. Aspirin treatment also increased the phosphorylation level of Bcl-XL, which might also contribute to aspirin-induced oncosis (Fig. 6a). Intriguingly, the remarkably increased level of total Bcl-XL at 24 h after aspirin treatment (Fig. 6a) might be due to cells stress response.

Our data that overexpression of Bax/Bad remarkably promotes aspirin-induced ATP depletion (Fig. 6b) and cells bubbling (Fig. 4) suggest that Bax/Bad promotes aspirin-induced oncosis likely by increasing ATP depletion. It was reported that BH3 domain of Bad formed a α helix upon binding to the hydrophobic groove on the surface of Bcl-XL protein [58]. Moreover, the small molecule inhibitor ABT-737, a mimetic of Bad, also binds to the BH3-binding domain groove of Bcl-XL [50]. Furthermore, binding of Bcl-XL to the β-subunit of the F_1F_0 ATP synthase can be reversed by ABT-737, suggesting that the ABT-737 binding region is needed for Bcl-XL binding to the β-subunit [35]. Our recent study demonstrated the strong binding of Bad to Bcl-XL to form heterodimer on mitochondria [59], which is further verified by our data that YFP-Bad has a good colocation with CFP-Bcl-XL (Fig. 4a, d). It is reasonable to infer that Bad promotes aspirin-induced oncosis by antagonizing Bcl-XL-β-subunit binding and reducing ATP synthesis.

Our evidences demonstrate that a minority of A549 cells undergo apoptosis after aspirin treatment. (1) There were about 10% of A549 cells died without the characteristic of bubbling (Fig. 2b); (2) In contrast to the complete contribution of CFP-Bax or YFP-Bad to the aspirin-induced bubbling in Hela cells (Fig. 4a), in the A549 cells expressing CFP-Bax or YFP-Bad, apoptotic cells significantly increased (Fig. 4d); (3) In contrast to the complete bubbling characteristic of dead cells induced by aspirin treatment for 12 h in Hela cells cultured in glucose-free DMEM medium, some dead cells without bubbling characteristic were observed in A549 cells after aspirin treatment for 18 h (Supplementary Fig. 3). Therefore, modest caspase-3 cleavage after aspirin treatment for 12 h in A549 cells was due to the apoptotic cells (Fig. 3b), which was further verified by the fact that Z-DEVD-FMK pretreatment significantly inhibited the aspirin-induced cytotoxicity (Fig. 3e). Moreover, Z-DEVD-FMK pretreatment significantly increased the aspirin-induced cells bubbling in A549 cells (Fig. 3f, Supplementary Fig. 2c), which must be due to the inhibition of caspase-3 and thus turnover of apoptosis to oncosis.

Obviously, Hela cells are more prone undergo oncosis than A549 cells during aspirin treatment. In keeping with this, aspirin treatment for 12 h induced a 13% of Hela cells bubbling and only 2% of A549 cells bubbling (Fig. 2b). In addition, aspirin treatment for 12 h induced a 36% of bubbling cells in Hela cells cultured in the glucose-free DMEM medium (Fig. 5d) and did not obviously induce cells bubbling in A549 cells. The reasons why Hela cells are more prone to undergo oncosis may be the following two points: (1) The endogenous Bcl-XL level of Hela cells is lower than that in A549 cells (Fig. 6a), thus A549 cells would possess stronger ability to maintain intracellular ATP level, which is consistent with our other data that the relative ATP level in A549 cells is higher than that in Hela cells after aspirin treatment for 12 h (Fig. 5a, b); (2) The endogenous pro-caspase-3 level in Hela cells is lower than that in A549 cells (Fig. 3b), thus A549 cells are more likely to undergo apoptosis, which is further verified by our data that Z-DEVD-FMK pretreatment significantly increased the aspirin-induced cells bubbling in A549 cells (Fig. 3f, Supplementary Fig. 2c).

Our data that the endogenous level of Bcl-XL in A549 cells is higher than that in human normal hepatocyte (LO2 cells) and Hela cells (Supplementary Fig. 4d) and Hela cells are more prone to bubbling than LO2 and A549 cells (Supplementary Fig. 1f) further verify the notion that the lower the endogenous Bcl-XL, the easier the cells bubble during aspirin treatment. It is reported that normal cells has lower endogenous Bcl-XL level than tumor cells [60], which may be the reason why normal cells were more prone undergo oncosis than some tumor cells with high level of endogenous Bcl-XL. The difference between tumor cells and non-tumor cells provides an alternative strategy for clinical treatment of tumors. In fact, aspirin also induced ATP depletion (Supplementary Fig. 1i) and oncosis (Supplementary Fig. 1e–h) in LO2 cells, in which declined Bcl-XL level was also critical (Supplementary Fig. 1j and Supplementary Fig. 4b, c).

Although there are many reports about induction of tumor cells death by high concentrations of aspirin (20 mM and 40 mM) [19, 61], 8–16 mM aspirin is an extremely high concentration and can hardly be achieved with normal aspirin intake [17, 62]. It was also reported that the cumulative dosage was determinant for the efficacy of aspirin on tumor inhibition [18]. Since tumor cells were treated with aspirin once, we adopted a high concentration of aspirin for our experimental system. The physiological and clinical meanings of the current study are that high concentration of aspirin may be used clinically for tumor inhibition by directly injecting aspirin into the tumor site instead of taking it orally. Rogério et al. [63] intratumorally injected of 10% bicarbonate aspirin solution to rabbits that were inoculated with VX2 hepatic tumor cells, and found that intralesional injection of a 10% aspirin solution caused destruction of VX2 hepatic tumors. Ouyang and co-workers [64] intratumorally injected NO-aspirin to mice that bore subcutaneous xenotransplants of HT-29 human colon cancer cells, and found that NO-aspirin suppressed the expression of VEGF, which led to suppressed angiogenesis against colon cancer.

In conclusion, this is the first report on aspirin-induced tumor cells oncosis. Decreased Bcl-XL level and subsequent intracellular ATP depletion dominate the aspirin-induced oncosis in which caspase-3 is not involved. Moreover, aspirin treatment inhibits EMT6 tumors growth and induces compromised level of Bcl-XL and ATP in tumor. Aspirin is more likely to induce oncosis in some specific tumor cell lines, such as Hela cells, with low level of both Bcl-XL and caspase-3, providing an alternative strategy for clinical treatment of tumors. Further investigation of aspirin-induced oncosis pathway should be helpful for optimizing the efficacy of aspirin-induced elimination of tumor cells.

Acknowledgements This work was supported by the National Natural Science Foundation of China (Grant Nos. 61875056, 61527825 and 81572184).

Author contributions LW, ZHM, XPW and TSC conceived and designed the study. LW, MXZ and TSC wrote the manuscript. LW, ZHM, MXZ and BW performed the experiments. LW, ZHM, MXZ, BW, SY, XPW and TSC analyzed and interpreted the data. All authors discussed, read and approved the final manuscript.

Compliance with ethical standards

Conflict of interest The authors declare that they have no conflict of interest.

References

1. Weissmann G (1991) Aspirin. Sci Am 264:84–90. https://doi.org/10.1038/scientificamerican0191-84
2. Fuster V, Sweeny JM (2011) Aspirin: a historical and contemporary therapeutic overview. Circulation 123:768–778. https://doi.org/10.1161/CIRCULATIONAHA.110.963843
3. Elwood PC, Cochrane AL, Burr ML, Sweetnam PM, Williams G, Welsby E et al (1974) A randomized controlled trial of acetyl salicyclic acid in the secondary prevention of mortality from myocardial infarction. Br Med J 1:436. https://doi.org/10.1136/bmj.1.5905.436
4. Fields WS, Lemak NA, Frankowski RF, Hardy RJ (1977) Controlled trial of aspirin in cerebral ischemia. Inpharma 98:10. https://doi.org/10.1007/BF03285461
5. International Stroke Trial (IST) (1997) A randomised trial of aspirin, subcutaneous heparin, both, or neither among 19435 patients with acute ischaemic stroke. International Stroke Trial Collaborative Group. Lancet 349:1569–1581. https://doi.org/10.1016/S0140-6736(97)04011-7
6. Chen ZM (1997) CAST: randomised placebo-controlled trial of early aspirin use in 20 000 patients with acute ischaemic stroke. Lancet 349:1641–1649. https://doi.org/10.1016/S0140-6736(97)04010-5
7. Johannesdottir SA, Chang ET, Mehnert F, Schmidt M, Olesen AB, Sørensen HT (2012) Nonsteroidal anti-inflammatory drugs

and the risk of skin cancer. Cancer 118:4768–4776. https://doi.org/10.1002/cncr.27406
8. Cao Y, Nishihara R, Wu K, Wang M, Ogino S, Willett WC et al (2016) Population-wide impact of long-term use of aspirin and the risk for cancer. JAMA Oncol 2:762–769. https://doi.org/10.1001/jamaoncol.2015.6396
9. Elwood PC, Morgan G, Pickering JE, Galante J, Weightman AL, Morris D et al (2016) Aspirin in the treatment of cancer: reductions in metastatic spread and in mortality: a systematic review and meta-analyses of published studies. PLoS ONE 11:e0152402. https://doi.org/10.1371/journal.pone.0152402
10. Tan XL, Lombardo KMR, Bamlet WR, Oberg AL, Robinson DP, Anderson KE et al (2011) Aspirin, nonsteroidal anti-inflammatory drugs (NSAID), acetaminophen, and pancreatic cancer risk: a clinic-based case-control study. Cancer Prev Res 4:1835. https://doi.org/10.1158/1940-6207.CAPR-11-0146
11. Cha YI, DuBois RN (2007) NSAIDs and cancer prevention: targets downstream of COX-2. Annu Rev Med 58:239–252. https://doi.org/10.1146/annurev.med.57.121304.131253
12. Liao X, Lochhead P, Nishihara R, Morikawa T, Yamauchi A et al (2012) Aspirin use, tumor PIK3CA mutation, and colorectal-cancer survival. N Engl J Med 367:1596–1606. https://doi.org/10.1056/NEJMoa1207756
13. Roelofs HM, Morsche RHT, Heumen BWV, Nagengast FM, Peters WH (2014) Over-expression of COX-2 mRNA in colorectal cancer. BMC Gastroenterol 14:9005. https://doi.org/10.1186/1471-230X-14-1
14. Ogawa F, Amano H, Ito Y, Matsui Y, Hosono K, Kitasato H et al (2014) Aspirin reduces lung cancer metastasis to regional lymph nodes. Biomed Pharmacother 68:79–86. https://doi.org/10.1016/j.biopha.2013.11.006
15. Hanif R, Pittas A, Feng Y, Koutsos MI, Qiao L, Staiano-Coico L et al (1996) Effects of nonsteroidal anti-inflammatory drugs on proliferation and on induction of apoptosis in colon cancer cells by a prostaglandin-independent pathway. Biochem Pharmacol 52:237–245. https://doi.org/10.1016/0006-2952(96)00181-5
16. Rigas B, Shiff SJ (2000) Is inhibition of cyclooxygenase required for the chemopreventive effect of NSAIDs in colon cancer? A model reconciling the current contradiction. Med Hypotheses 54:210–215. https://doi.org/10.1054/mehy.1999.0023
17. Stark LA, Din FVN, Zwacka RM, Dunlop MG (2001) Aspirin-induced activation of the NF-κB signaling pathway: a novel mechanism for aspirin-mediated apoptosis in colon cancer cells. FASEB J 15:1273–1275. https://doi.org/10.1096/fj.00-0529fje
18. Chen ZG, Li WL, Qiu FM, Huang Q, Jiang Z, Ye J et al (2018) Aspirin cooperates with p300 to activate the acetylation of H3K9 and promote FasL-mediated apoptosis of cancer stem-like cells in colorectal cancer. Theranostics 8:4447–4461. https://doi.org/10.7150/thno.24284
19. Redlak MJ, Power JJ, Miller TA (2005) Role of mitochondria in aspirin-induced apoptosis in human gastric epithelial cells. Am J Physiol Gastr L 289:G731–G738. https://doi.org/10.1152/ajpgi.00150.2005
20. Gu Q, Wang JD, Xia HH, Lin MC, He H, Zou B et al (2005) Activation of the caspase-8/Bid and Bax pathways in aspirin-induced apoptosis in gastric cancer. Carcinogenesis 26:541–546. https://doi.org/10.1093/carcin/bgh345
21. Zimmermann KC, Waterhouse NJ, Goldstein JC, Schuler M, Green DR (2000) Aspirin induces apoptosis through release of cytochrome c from mitochondria. Neoplasia 2:505–513. https://doi.org/10.1038/sj.neo.7900120
22. Din FVN, Valanciute A, Houde VP, Zibrova D, Green KA, Sakamoto K et al (2012) Aspirin inhibits mTOR signaling, activates AMP-activated protein kinase, and induces autophagy in colorectal cancer cells. Gastroenterology 142:1504–1515. https://doi.org/10.1053/j.gastro.2012.02.050
23. Yue W, Yang CS, Dipaola RS, Tan XL (2014) Repurposing of metformin and aspirin by targeting AMPK-mTOR and inflammation for pancreatic cancer prevention and treatment. Cancer Prev Res 7:388–397. https://doi.org/10.1158/1940-6207.CAPR-13-0337
24. Jaeschke H, Lemasters JJ (2003) Apoptosis versus oncotic necrosis in hepatic ischemia/reperfusion injury. Gastroenterology 125:1246–1257. https://doi.org/10.1016/S0016-5085(03)01209-5
25. Degterev A, Yuan J (2008) Expansion and evolution of cell death programmes. Nat Rev Mol Cell Bio 9:378. https://doi.org/10.1038/nrm2393
26. Berghe TV, Vanlangenakker N, Parthoens E, Deckers W, Devos M, Festjens N et al (2010) Necroptosis, necrosis and secondary necrosis converge on similar cellular disintegration features. Cell Death Differ 17:922. https://doi.org/10.1038/cdd.2009.184
27. Cooley-Andrade O, Goh WX, Connor DE, Ma DD, Parsi K (2016) Detergent sclerosants stimulate leukocyte apoptosis and oncosis. Eur J Vasc Endovasc Surg 51:846–856. https://doi.org/10.1016/j.ejvs.2016.03.008
28. Weerasinghe P, Buja LM (2012) Oncosis: an important non-apoptotic mode of cell death. Exp Mol Pathol 93:302–308. https://doi.org/10.1016/j.yexmp.2012.09.018
29. Del NC, Xiao Y, Rangell L, Reichelt M, O'Brien T (2014) Depletion of the central metabolite NAD leads to oncosis mediated cell death. J Biol Chem 289:35182. https://doi.org/10.1074/jbc.M114.580159
30. Peters AA, Syn J, Ktds Y, Chalmers S, Wiegmans AP, Lim HF et al (2017) Oncosis and apoptosis induction by activation of an overexpressed ion channel in breast cancer cells. Oncogene 36:6490. https://doi.org/10.1038/onc.2017.234
31. Leist M, Single B, Castoldi AF, Kühnle S, Nicotera P (1997) Intracellular adenosine triphosphate (ATP) concentration: a switch in the decision between apoptosis and necrosis. J Exp Med 185:1481–1486. https://doi.org/10.1084/jem.185.8.1481
32. Kon K, Kim JS, Jaeschke H, Lemasters JJ (2004) Mitochondrial permeability transition in acetaminophen-induced necrosis and apoptosis of cultured mouse hepatocytes. Hepatology 40:1170–1179. https://doi.org/10.1002/hep.20437
33. Knight TR, Jaeschke H (2002) Acetaminophen-induced inhibition of Fas receptor-mediated liver cell apoptosis: mitochondrial dysfunction versus glutathione depletion. Toxicol Appl Pharmacol 181:133–141. https://doi.org/10.1006/taap.2002.9407
34. Garciabelinchón M, Sánchezosuna M, Martínezescardó L, Granadoscolomina C, Pascualguiral S, Iglesiasguimarais V et al (2015) An early and robust activation of caspases heads cells for a regulated form of necrotic-like cell death. J Biol Chem 290:20841–20855. https://doi.org/10.1074/jbc.M115.644179
35. Alavian KN, Li H, Collis L, Bonanni L, Zeng L, Sacchetti S et al (2011) Bcl-XL regulates metabolic efficiency of neurons through interaction with the mitochondrial F_1F_O ATP synthase. Nat Cell Biol 13:1224. https://doi.org/10.1038/ncb2330
36. Kane DJ, Ord T, Anton R, Bredesen DE (1995) Expression of bcl-2 inhibits necrotic neural cell death. J Neurosci Res 40:269–275. https://doi.org/10.1002/jnr.490400216
37. Bajt ML, Farhood A, Lemasters JJ, Jaeschke H (2008) Mitochondrial bax translocation accelerates DNA fragmentation and cell necrosis in a murine model of acetaminophen hepatotoxicity. J Pharmacol Exp Ther 324:8–14. https://doi.org/10.1124/jpet.107.129445
38. Mills EM, Xu D, Fergusson MM, Combs CA, Xu Y, Finkel T (2002) Regulation of cellular oncosis by uncoupling protein 2. J Biol Chem 277:27385–27392. https://doi.org/10.1074/jbc.M111860200
39. Liu X, Schnellmann RG (2003) Calpain mediates progressive plasma membrane permeability and proteolysis of cytoskeleton-associated paxillin, talin, and vinculin during renal cell death.

J Pharmacol Exp Ther 304:63–70. https://doi.org/10.1124/jpet.102.043406
40. Liu X, Van VT, Schnellmann RG (2004) The role of calpain in oncotic cell death. Annu Rev Pharmacol Toxicol 44:349–370. https://doi.org/10.1146/annurev.pharmtox.44.101802.121804
41. Weerasinghe P, Hallock S, Tang SC, Trump B, Liepins A (2006) Sanguinarine overcome P-glycoprotein-mediated mult idrug-resistance vi ainduction of apoptosis and oncosis in CEM-VLB 1000 cells. Exp Toxicol Pathol 58:21–30. https://doi.org/10.1016/j.etp.2006.01.008
42. Qin G, Wu L, Liu H, Pang Y, Zhao C, Wu S et al (2015) Artesunate induces apoptosis via a ROS-independent and Bax-mediated intrinsic pathway in HepG2 cells. Exp Cell Res 336:308–317. https://doi.org/10.1016/j.yexcr.2015.07.004
43. Perelman A, Wachtel C, Cohen M, Haupt S, Shapiro H, Tzur A (2012) JC-1: alternative excitation wavelengths facilitate mitochondrial membrane potential cytometry. Cell Death Dis 3:e430. https://doi.org/10.1038/cddis.2012.171
44. Klee M, Pimentel-Muiños FX (2005) Bcl-XL specifically activates Bak to induce swelling and restructuring of the endoplasmic reticulum. J Cell Biol 168:723–734. https://doi.org/10.1083/jcb.200408169
45. Pang Y, Qin G, Wu L, Wang X, Chen T (2016) Artesunate induces ROS-dependent apoptosis via a Bax-mediated intrinsic pathway in Huh-7 and Hep3B cells. Exp Cell Res 347:251–260. https://doi.org/10.1016/j.yexcr.2016.06.012
46. Trump BE, Berezesky IK, Chang SH, Phelps PC (1997) The pathways of cell death: oncosis, apoptosis, and necrosis. Toxicol Pathol 25:82–88. https://doi.org/10.1177/019262339702500116
47. Chen YB, Aon MA, Hsu YT, Soane L, Teng X, McCaffery JM et al (2011) Bcl-XL regulates mitochondrial energetics by stabilizing the inner membrane potential. J Cell Biol 195:263–276. https://doi.org/10.1083/jcb.201108059
48. Alavian KN, Beutner G, Lazrove E, Sacchetti S, Park H, Licznerski P et al (2014) An uncoupling channel within the c-subunit ring of the F_1F_0 ATP synthase is the mitochondrial permeability transition pore. Proc Natl Acad Sci USA 111:10580–10585. https://doi.org/10.1073/pnas.1401591111
49. McNally MA, Soane L, Roelofs BA, Hartman AL, Hardwick JM (2013) The N-terminal helix of Bcl-XL targets mitochondria. Mitochondrion 13:119–124. https://doi.org/10.1016/j.mito.2013.01.004
50. Hickman JA, Hardwick JM, Kaczmarek LK, Jonas EA (2008) Bcl-XL inhibitor ABT-737 reveals a dual role for Bcl-XL in synaptic transmission. J Neurophysiol 99:1515–1522. https://doi.org/10.1152/jn.00598.2007
51. Alfonso L, Ai G, Spitale RC, Bhat GJ (2014) Molecular targets of aspirin and cancer prevention. Br J Cancer 111:61. https://doi.org/10.1038/bjc.2014.271
52. Jana NR (2008) NSAIDs and apoptosis. Cell Mol Life Sci 65:1295–1301. https://doi.org/10.1007/s00018-008-7511-x
53. Weerasinghe P, Hallock S, Tang SC, Liepins A (2001) Role of Bcl-2 family proteins and caspase-3 in sanguinarine-induced bimodal cell death. Cell Biol Toxicol 17:371. https://doi.org/10.1023/A:101379643
54. Chiarugi A (2005) "Simple but not simpler": toward a unified picture of energy requirements in cell death. FASEB J 19:1783–1788. https://doi.org/10.1096/fj.05-4200rev
55. Nicotera P, Melino G (2004) Regulation of the apoptosis–necrosis switch. Oncogene 23:2757. https://doi.org/10.1038/sj.onc.1207559
56. Khandelwal N, Simpson J, Taylor G, Rafique S, Whitehouse A, Hiscox J (2011) Nucleolar NF-κB/RelA mediates apoptosis by causing cytoplasmic relocalization of nucleophosmin. Cell Death Differ 18:1889. https://doi.org/10.1038/cdd.2011.79
57. Del Re DP, Matsuda T, Zhai P, Maejima Y, Jain MR, Liu T et al (2014) Mst1 promotes cardiac myocyte apoptosis through phosphorylation and inhibition of Bcl-XL. Mol Cell 54:639–650. https://doi.org/10.1016/j.molcel.2014.04.007
58. Martinou JC, Youle RJ (2011) Mitochondria in apoptosis: Bcl-2 family members and mitochondrial dynamics. Dev Cell 21:92–101. https://doi.org/10.1016/j.devcel.2011.06.017
59. Du M, Yang F, Mai Z, Qu W, Lin F, Wei L (2018) FRET two-hybrid assay by linearly fitting FRET efficiency to concentration ratio between acceptor and donor. Appl Phys Lett 112:153702. https://doi.org/10.1063/1.5021466k
60. Gobé G, Rubin M, Williams G, Sawczuk I, Buttyan R (2002) Apoptosis and expression of Bcl-2, Bcl-XL, and Bax in renal cell carcinomas. Cancer Invest 20:9. https://doi.org/10.1081/CNV-120001177
61. Subbegowda R, Frommel TO (1998) Aspirin toxicity for human colonic tumor cells results from necrosis and is accompanied by cell cycle arrest. Cancer Res 58:2772–2776
62. Ahmed N, Meek J, Davies GJ (2010) Plasma salicylate level and aspirin resistance in survivors of myocardial infarction. J Thromb Thrombolys 29:416–420. https://doi.org/10.1007/s11239-009-0366-7
63. Rogério SH, Fábio VT, Denadai R (2013) In vivo assessment of intratumoral aspirin injection to treat hepatic tumors. World J Hepatol 5:372–378. https://doi.org/10.4254/wjh.v5.i7.372
64. Ouyang N, Williams JL, Rigas B (2008) NO-donating aspirin inhibits angiogenesis by suppressing VEGF expression in HT-29 human colon cancer mouse xenografts. Carcinogenesis 29:1794–1798. https://doi.org/10.1093/carcin/bgn127